A Monolithic Diode Array Millimeter-Wave Beam Transmittance Controller

Lance B. Sjogren, Hong-Xia L. Liu, Feng Wang, Tina Liu, Xiao-Hui Qin, Wenhsing Wu, Esther Chung, Calvin W. Domier, N. C. Luhmann, Jr.

Abstract— **Amplitude control of transmitted millimeter-wave beams by monolithic Schottky diode arrays is demonstrated. An array containing 4800 diodes has demonstrated control over the range 20–50% beam transmittance at 99 GHz and 20–70% beam transmittance at 165 GHz. Modulation testing on a second array (8640 diodes) with similar transmission characteristics has shown array control to 50 MHz with negligible loss of output response. An extensive evaluation performed for the 8640 diode array shows good agreement between array impedance parameters determined from quasi-optical measurements, theoretical calculations, and low frequency C-V measurements. The results have extended the range of quasi-optical functions demonstrated by solid-state power-combining arrays for application to millimeter-wave systems.**

I. Introduction

QUASI-OPTICAL PROPAGATION is gaining increasing favor as a waveguiding mechanism for millimeter-wave electronic systems. By the spatial combining of the output from large arrays of low-power semiconductor devices, originally proposed in [1], quasi-optical arrays are capable of operating at substantial power levels. Quasi-optical "waveguiding" exhibits significantly lower Ohmic losses than metallic waveguide or microstrip, with concomitant gains in efficiency. In addition, while microstrip circuits suffer large increases in radiative losses with increasing frequency, radiative (spillover) losses of quasi-optical circuits decrease with increasing frequency for a given beam size.

To create quasi-optical counterpart systems to those previously developed in waveguide or microstrip, the family of required components must be implemented in quasi-optical form. Substantial progress has recently been reported toward that end. Monolithic diode grids have demonstrated phase shifting at 93 GHz [2], frequency doubling from 33 to 66 GHz [3], and frequency tripling from 33 to 99 GHz [4]. One-dimensional monolithic imaging arrays have been demonstrated at 94 GHz [5]. Additional quasi-optical functions have been demonstrated at microwave frequencies by arrays employing hybrid technology. These include the oscillator grid [6]–[8], amplifier grid [9], and mixer grid [10]. In addition, small arrays of more complex quasi-optical elements (e.g. injection-locked FET oscillators [11]) have been demonstrated.

Diode arrays for microwave power switching in rectangular waveguide have existed for over two decades [12]. Very recently, quasi-optical counterparts have been developed. The concept of employing a Schottky varactor diode array as a beam transmittance controller was originally proposed in [13], and subsequently experimentally demonstrated by a monolithic array [14]. Reflected/transmitted beam switching by a hybrid p-i-n diode array has been recently demonstrated, as well [15].

In the current work, a detailed examination is made of the performance of the monolithic Schottky diode beam transmission controller. Power transmittance as a function of array bias is presented for arrays of 4800 and 8640 diodes. An extensive characterization is performed for the 8640 diode array. Based on experimental results, low frequency device parameters, and circuit simulations, two models have been developed which characterize the array behavior. First, a model for the impedance of the array with respect to the millimeter-wave beam has been devised. This impedance determines the extent of the array's beam transmission control behavior. Second, a model for the impedance of the array with respect to the control (bias) input signal has been devised. This impedance determines the array's ability to be operated at high control speed. The models should assist in the systematic design of new, higher performance, arrays.

II. Beam Transmission Control

A. Transmission Results

The basic operation of the array can be explained by the quasi-optical plane wave approximation. A millimeter-wave beam incident upon the array is represented as a TEM wave propagating on a transmission line whose propagation constant is $k = \omega\sqrt{\mu\varepsilon}$ and whose characteristic impedance is $\eta = \sqrt{\mu/\in}$. A periodic (in the transverse plane) array placed in the path of the beam can be treated as a shunt impedance across the quasi-optical transmission line. For the Schottky varactor diode array, this impedance can be tuned by diode bias voltage.

The array utilized in the current work consists of a periodic grid containing thousands of monolithically integrated diodes. It is fabricated by a self-aligned Aluminum Schottky diode process [5]. The starting material consists of a semi-insulating Gallium Arsenide wafer with a Molecular Beam Epitaxially

Manuscript revised March 18, 1993.

The authors are or were with the Department of Electrical Engineering, University of California, Los Angeles 90024-1594.

L. B. Sjogren is now with TRW ETD, Redondo Beach, CA.

H.-X. L. Liu is now with Loral Space/Systems Palo Alto, CA.

W. Wu, is now with Silicon Systems, Tustin, CA.

IEEE Log Number 9211916.

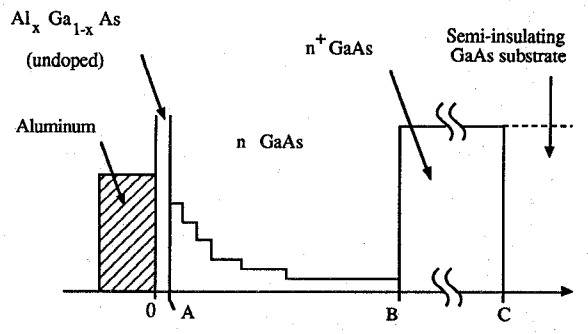

Fig. 1. Epitaxial profile for the beam control arrays. The profile is shown as a function of depth (angstroms) into the semiconductor. The A1 "cap" layer is 2000 Å. The values of the indicated parameters are $x = 0.5$, $A = 200$ Å, $B = 4000$ Å, $C = 14,000$ Å, n^+ doping—3×10^{18} cm^{-3}, n GaAs doping—150 Å at 5×10^{17} cm^{-3}, 100 Å at 4×10^{17} cm^{-3}, 150 Å at 3×10^{17} cm^{-3}, 250 Å at 2×10^{17} cm^{-3}, 350 Å at 1.5×10^{17} cm^{-3}, 500 Å at 1.0×10^{17} cm^{-3}, 700 Å at 7.5×10^{16} cm^{-3}, and 1600 Å at 5.0×10^{16} cm^{-3}.

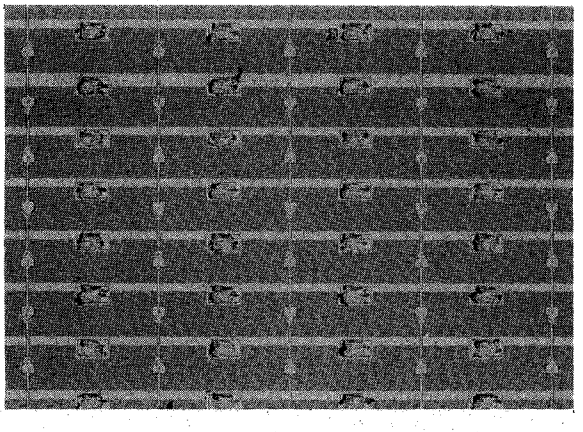

Fig. 2. Photograph of a local array region. Unit cell dimensions are width $(a) = 300$ μm and height $(b) = 120$ μm. The marks on the large pads are from automated testing of the individual diodes. The array operates on a beam whose electric field is oriented in the vertical (y) direction.

(MBE) grown layer as shown in Fig. 1. A widegap "blocking barrier" [16] is employed to suppress thermionic current in forward bias and tunneling current in reverse bias. Device isolation is performed by a two-step proton implantation (4×10^{14} cm^{-2} at 200 keV and 4×10^{14} cm^{-2} at 100 keV), with an implantation mask of thick photoresist (Hoechst AZP4620). The physical structure of the array is illustrated by the microscope photograph of Fig. 2. The array unit cell dimensions are 300 μm by 120 μm. As defined by the photomasks, the diode embedding strip is 7 μm wide, and the diode is 3 μm by 13 μm. (Simulations indicated this set of dimensions should provide a large array impedance range.) Diode orientation is alternated along the vertical axis to allow use of a common ground connection. Perpendicular (horizontal) strips provide bias voltage to the diodes. The large pads on the bias strip allow automated probing/I-V testing of the individual array diodes prior to application of the final bias metallization.

The two arrays examined in this work possessed usable areas containing 4800 and 8640 diodes, respectively. For both arrays, approximately 2% of the diodes were short-circuited. The short circuits were eliminated by microprobe cutting. In addition, some diodes (2% at most) possessed open circuits.

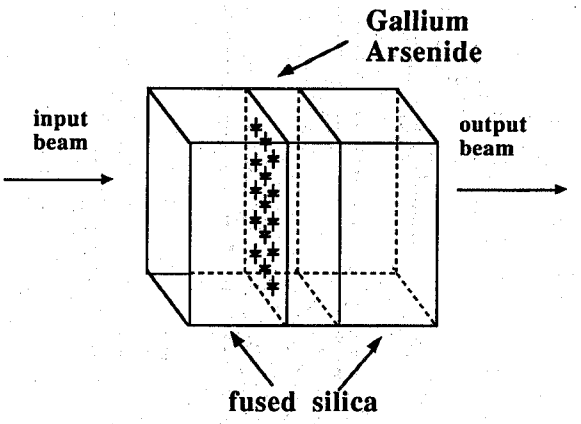

Fig. 3. Stacking configuration for transmission testing of the array. Array thickness is 0.635 mm. Fused silica plate thickness is 1.16 mm. These thicknesses both correspond to $3\lambda/4$ at 99 GHz.

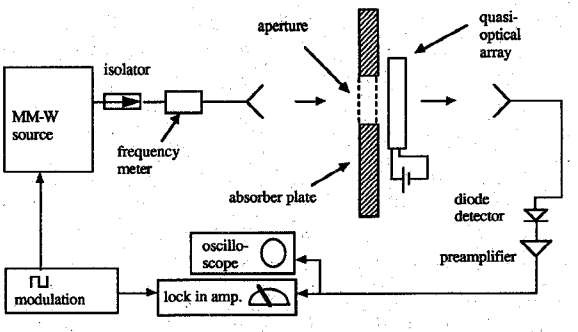

Fig. 4. Quasi-optical system for measurement of transmitted beam amplitude. With the array stack removed, a reference beam of unity transmittance is measured.

Thus, over 96% of the diodes in the usable areas were functional. Most of the short-circuited diodes appear to have been faulty due to electrical overstress during testing. This problem appears to have been subsequently eliminated by the addition of a 100 kΩ resistor in series with the diode in the test system.

Although the beam control array alone can be employed to perform transmittance control, the performance can be improved by including additional dielectric layers. In the current work, fused silica plates were placed above and below the array to serve as reflection-reducing impedance transformers (see Fig. 3).

The configuration for transmitted beam testing is shown in Fig. 4. The 4800 diode array was tested for beam transmittance in the W (75 GHz–110 GHz) and D (110–170 GHz) frequency bands. Fig. 5 shows the measured power transmittance at three frequencies. The form of these curves can be explained by the fact that the array behaves as a series RLC circuit. The resistance and capacitance are due to the diode and the inductance is due to the diode embedding strip. The transmittance behavior at 99 GHz, 132 GHz, and 165 GHz illustrate the capacitive, resonant, and inductive conditions, respectively, of the RLC circuit. The results show that the array has two useful frequency "bands" for transmittance control, a lower frequency (capacitive) band and a higher frequency (inductive) band.

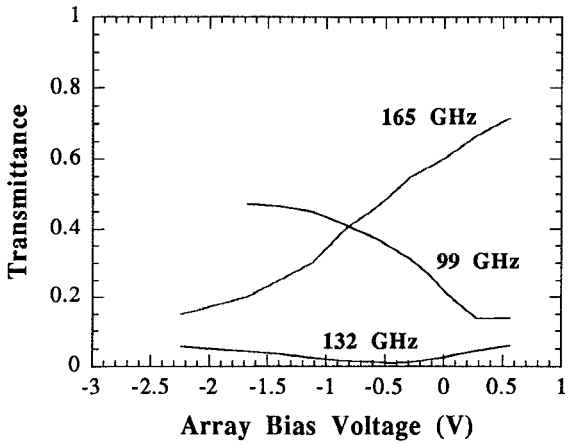

Fig. 5. Transmission test results for the 4800 diode array.

The 8640 diode array, fabricated concurrently with the 4800 diode array, showed similar results for transmittance versus bias and frequency. Additional tests were performed on the 8640 device array to measure the quasi-optical transmitted phase and input (bias) control speed. The results of these measurements have been compared to theoretical and low-frequency measurement results to provide an extensive characterization of both the quasi-optical and control behavior of the array. The details of this characterization are given in the remainder of this paper.

III. Array Characterization

A. Theoretical/Low Frequency Parameters

In order to more fully characterize the behavior of the diode array, simulations have been performed to predict the array's impedance parameters. Additional simulations have been performed to predict the diode characteristics. Furthermore, low frequency diode C-V test have been made as a "bridge" between the originally simulated results and the millimeter-wave experimental results. In this section, the details of the simulations and low frequency tests are discussed.

The quasi-optical impedance of the array can be represented by the small-signal circuit shown schematically in Fig. 6. This is based, with some extensions, on that of [17]. Note that the diode impedance elements scale according to the unit cell shape, since there are a/b diodes "in-series" in a square $Z_0 = \eta(\eta = \sqrt{\mu/\varepsilon})$ equivalent TEM waveguide.

Due to the symmetry of the array structure, the horizontal (bias) strip and the vertical diode-embedded strip are quasi-optically independent. The horizontal strip behaves as a capacitive grid; it is represented by the element C_{bias}. Finite element analysis performed with a commercial electromagnetic simulation program (Hewlett Packard High Frequency Structure Simulator-HFSS) [18] gives a capacitance of 2.3 fF. (This capacitance will change if a superstrate is present on the array, however.) Since this capacitance is not part of the series RLC structure formed by the diode and its embedding strip, it is not a primary factor in determining the millimeter-wave behavior of the array.

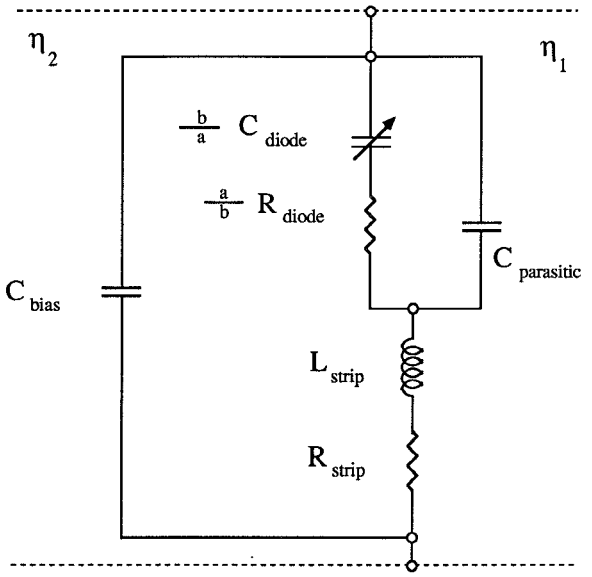

Fig. 6. Equivalent circuit for the diode array.

The vertical embedding strip constitutes an inductive grid, with inductance and resistance denoted by L_{strip} and R_{strip}, respectively. A narrow (7 μm drawn, 8 μm actual) strip has been employed to provide a large maximum inductive reactance. Predicted values of array inductance were obtained by use of the diode array impedance model [17], a quasistatic formula [19], and HFSS. The values from the HFSS were about 10% lower than those from the other methods, but are probably more accurate due to less assumptions regarding the field distribution. This simulation gives a predicted value of 177 pH for the uniform strip. The strip resistance can be estimated from published curves [20] which account for the skin effect. For the 300 $\times$ 8 $\times$ 0.8 μm strip comprised primarily of gold, this yields $R_{strip} = 2.8\ \Omega$. This resistance constitutes less than 10% of that for the current arrays. However, it will become a more significant factor as diodes with lower resistance are achieved. Furthermore, the value of strip resistance will increase for array designs scaled to higher frequency. Geometric scaling should give the same DC resistance, but the skin depth will decrease for higher frequency. One approach to achieve very high efficiency in future designs is to employ high T_c superconducting material [21] for the embedding strip.

The element $C_{parasitic}$ can be considered the sum of a diode parasitic capacitance between anode and cathode, and an additional capacitance associated with the periodic grid structure [17]. The value of the latter (denoted C_{grid}) was calculated in [17], with comparable values obtained with the HFSS program. Simulations which do not include the effect of $C_{parasitic}$ indicates that a square array cell of 300 μm in size should provide a good array impedance range. However, the grid capacitance for such an array is calculated to be 4.5 fF. This is sufficiently large to substantially reduce the predicted impedance range of the array. Consequently, the effect has been suppressed by use of a "rectangular unit cell" [17]. With a unit cell of $a = 300\ \mu$m by $b = 120\ \mu$m, the estimated value of C_{grid} is approximately 1.0 fF. However, this value

is likely an underestimate of the parasitic capacitance, since it assumes an idealized shape for the metallization grid. A more rigorous simulation can be performed by including the actual two dimensional metallization pattern in an HFSS simulation. However, even this is not a rigorous approach, since the "screening" effect of the diode is not included. A rough estimate of the worst case parasitic capacitance was obtained by the following rationale: In some situations (e.g. phase shifting with large phase range), two arrays will be stacked together. In this case, the bottom array sees a Gallium Arsenide superstrate layer as well as substrate. The "screening" effect of the diode will reduce the parasitic capacitance on the substrate side, however. Thus, most of the capacitance will be associated with the fields in the superstrate layer. Consequently, simulation with a GaAs superstrate and air substrate should provide a rough estimate of the parasitic capacitance in this worst-case configuration. Such a simulation was performed with HFSS at two frequencies in order to extract both the capacitance and inductance. The result obtained was an inductance of 180 pH (in agreement with the result for the plain strip), and a capacitance of 3.8 fF. An additional simulation was performed with this metallization with a 300 μm by 300 μm unit cell. The diode size was scaled by a factor of $1/2.5$ to account for the shape factor of the impedance. The capacitance value obtained was 7.4 fF. These results suggest, once again, that the rectangular unit cell is effective in reducing parasitic capacitance.

The diode C-V characteristics were first evaluated by low frequency tests. This was done by cutting individual diodes from the array with a microprobe, and comparing the C-V characteristics before and after cutting. (Direct measurement of the diode capacitance gave erroneous values due to the large low frequency capacitance of the coplanar test pad/bias strips.) The C-V characteristics of an average sized diode are compared to those from the results of the initially-performed one-dimensional device simulation in Fig. 7. The values are scaled by b/a so that they represent the quasi-optical diode capacitance. The curves show that the effective size of the diode is less than predicted. (An "exact" value for the fractional shrinkage of the diode does not exist, however, because the theoretical and measured capacitance curves are not identical in shape.) The diode is designed for a width of 2 μm, based on a 3 μm Schottky contact and an expected undercut of 0.5 μm on each side. The results suggest that a much larger undercut occurred. This is plausible considering that in a previous design [5] such a diode with a drawn width of 3 μm was reduced to an effective size of 0.8 μm. The effective diode size may also be slightly reduced by the edge taper of the thick photoresist used as the isolation implant mask.

Even considering the reduced effective diode size, the maximum capacitance appears lower than expected. This may be largely due to a reduction in effective doping due to some penetration of isolation implant into the active device. A group of arrays whose edge was not completely isolated due to "edge bead" of the implant masking photoresist was implanted a second time, with a cumulative implant dose three times as high as that of the successful arrays. These arrays showed virtually no capacitance variation with bias after the second implant. This suggests that some of the implant is penetrating into the active diode area; hence, the effective doping concentration may be lower than that of the original epitaxial material. To compensate for this effect, a higher doping can be used in the doped region nearest the Schottky contact. If this change is made, however, the doping of the remainder of the n layer should be decreased. Increased doping will reduce the breakdown voltage, and the value achieved here for breakdown voltage of -4 to -5 V, was just sufficient to fully deplete the n region.

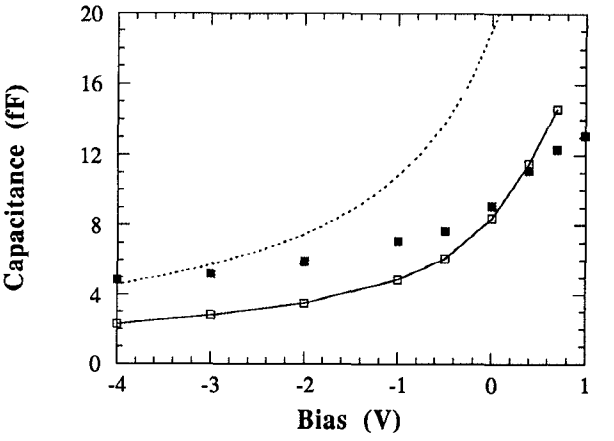

Fig. 7. C-V characteristics for the PS1 array. Dashed line- Original one-dimensional simulation. Solid line- measured 1 MHz C-V curve for typical array diode. Both curves are divided by the aspect ratio a/b for direct comparison with the quasi-optical C-V results, which are shown by solid markers.

The diode resistance consists of contributions due to the anode finger, undepleted region, n^+ region path from diode to Ohmic contact, and the Ohmic contact. The first three of these, based on simple uniform cross-section resistance formula calculations, are estimated to be 0.6 Ω, 1.75 Ω, and 1.5 Ω, respectively. A conservative (no fringing) prediction based on the transmission line model [22] gives 6.1 Ω per diode for the Ohmic contact resistance. Thus, the estimated diode resistance is approximately 10 Ω. Due to the wide-gap barrier layer, the diodes, unlike standard Schottky diodes, do not exhibit a sharp "turn-on" at a small forward bias. (These diodes have been biased to as high as +3.0V.) Consequently, measurements of diode resistance by the standard forward bias I-V test give erroneous results.

B. Experimentally-Determined Quasi-Optical Model

Based on the preceding calculations, the dominant elements of the circuit of Fig. 6 are the strip inductance, diode capacitance, and diode resistance. Thus, the array can approximately be represented as a series RLC circuit. To provide a comparison between the predicted and actual behavior of the array, experimental values of R, L, and C for this three-element model were extracted from the measured beam transmission results. The procedure employed was to determine the component values, which, when inserted into a transmission-line simulation of the quasi-optical circuit, provided the best agreement (least-squares fit) with the measured transmission curves. This was performed for the transmitted beam phase,

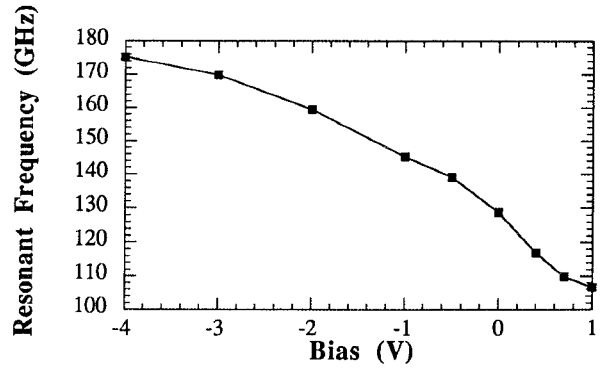

Fig. 8. Resonant frequency of the array versus bias. Markers indicate the experimentally-determined values.

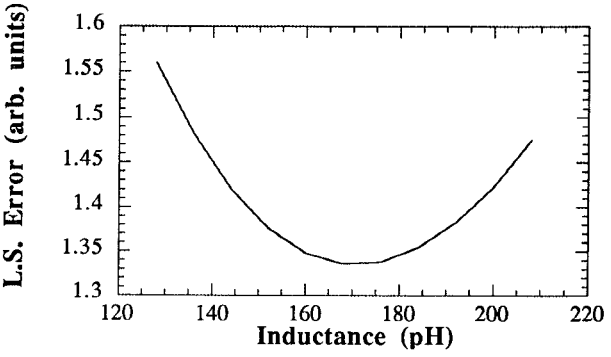

Fig. 9. Least-squares model fit versus inductance for the array.

which was measured by the method of [23]. The curve-fitting was performed with 90 data points (nine bias voltages over ten frequencies spanning D band).

For a wide range of simulated values for L and C, a best fit was obtained with $R = 40\ \Omega$. Bias-dependence of the resistance (due to the undepleted region resistance) was too small to be observed. The predicted value for the resistance is 28 Ω, based on a/b times the estimated diode resistance of 10 Ω, plus the estimated strip resistance of 3 Ω. Results from subsequent experiments indicate that the additional resistance is probably due to a greater than predicted anode finger resistance due to thinning of the Schottky contact metallization.

The resonant frequency $f_{res} = \left[2\pi\sqrt{LC}\right]^{-1}$ versus bias was not a strong function of the individual values of L and C. Consequently, $fres$ was easily determined by inspection of tables of simulated results. The result is shown in Fig. 8.

Quasi-optical inductance can be treated as a known quantity for a uniform embedding strip, but was treated here as an unknown because of the variation due to the wider metal at the Ohmic contact and bias strip. Fig. 9 shows the least squares error of the curves as a function of simulated inductance. This indicates that a best estimate for inductance is approximately 170 pH. This is in essential agreement with the value from HFSS simulation of 177 pH.

With the inductance and resonant frequency versus bias determined, the capacitance, C, of the series RLC array model is known. The quasi-optical C-V characteristics determined from the transmission measurements are shown in Fig. 7. The curve differs primarily from the low-frequency C-V curve in that the quasi-optical capacitance shows less bias-dependence. Several factors may contribute to this effect. First, the array possesses one bias unit (group of contiguous diode rows connected to a single bias line) at the center of the useable array area which cannot be biased, due to a short circuit. Although the array contained 18 useable bias units, the transmission tests were performed with an aperture sized for 10 bias units. Hence, the faulty unit comprises 10% of the active area. As mentioned previously, a few percent of the individual diodes were also inoperable. Furthermore, some of the bias units possess leakage currents at large forward or reverse bias. Under such conditions, not all of the bias appears at the diodes. (The rest appears across 220 Ω resistors placed in series with the diodes for overcurrent protection, and along the array bias strips.)

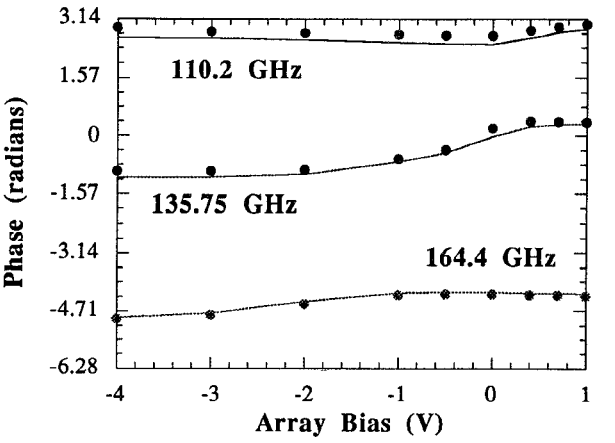

Fig. 10. Transmitted beam phase curves for the PS1 diode array. Markers indicate experimental results. Solid lines represent curves based on a quasi-optical circuit model which provide a "best-fit" with the measured curves.

With the best fit values of R, L, and C (V) chosen, the modeled curves can be plotted against the experimental curves. Three transmitted beam phase curves are shown in Fig. 10. As can be seen, a good fit is obtained for the series RLC model. Note that the method of [23] employs the (bias-independent and predictable) transmission phase of an orthogonally polarized beam as a reference. This provides a much more rigorous verification of the agreement between theory and experiment than that which would be obtained if a "phase offset" correction factor had been required. The corresponding transmittance curves are shown in Fig. 11. These show that the model determined from phase measurements correctly predicts the amplitude.

Using the experimentally-determined model, the frequency performance for maximum and minimum transmittance can be predicted outside the measured range, and is shown in Fig. 12. Outside the frequency range of the two primary transmittance control "bands", the graph suggests the presence of "minibands" at about 65 and 205 GHz, at which a substantial transmittance control should be possible.

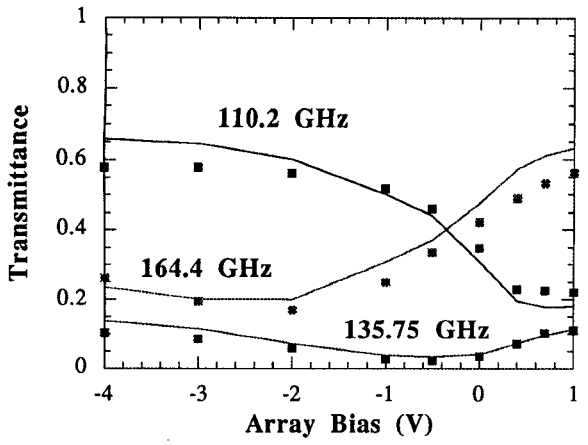

Fig. 11. Transmitted beam power curves for the PS1 array. Markers indicate experimental results. Solid lines represent curves based on a quasi-optical circuit model with "best fit" element values extracted from quasi-optical transmission coefficient phase measurements.

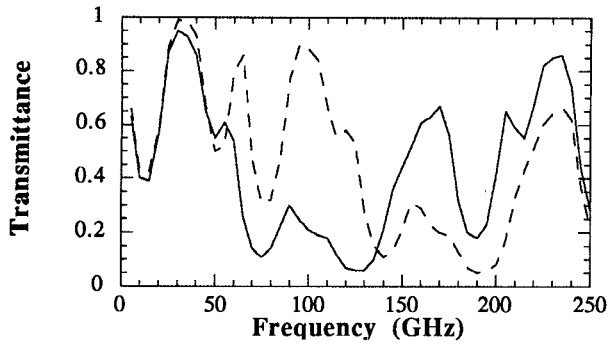

Fig. 12. Extrapolated maximum and minimum beam power versus frequency. The crossover between the capacitive and inductive regions can be seen to occur at approximately 137 GHz. Dashed line- transmittance at minimum (most negative) bias. Solid line- transmittance at maximum (most positive) bias.

A large-signal evaluation of the array has not been performed. However, some observations can be made regarding the power-handling capability of the array. Factors limiting operating power level include transfer to higher-order harmonics (frequency multiplication) and heat dissipation. It should be noted that the alternating diode orientation will result (ideally) in the absence of even harmonics. A simple estimate of the power-handling ability of the array can be obtained from a small-signal circuit analysis in which the input power and dissipated power are determined based on a conservative limit for AC voltage on the individual diodes. (The circuit simulated was the stack configuration of Fig. 3.) With a maximum peak AC voltage of 0.3 V on each diode, the input power limit is 1.8 mW at 110.2 GHz (capacitive band) and 0.5 mW at 164.4 GHz (inductive band) per diode cell. The more severe limitation, that at 164.4 GHz, results in an array power-handling capability of 1.4 W/cm^2, or 5 W for a 10,000 diode array. Considering the fact that the array is a small-signal device, this is a substantial power-handling ability. This ability is attributable to the high device density employed. The worst-case dissipated power as a percentage of input power is 20%

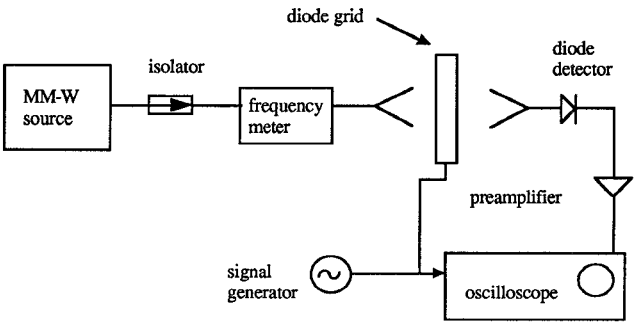

Fig. 13. Array modulation test system.

and 51%, respectively, at the frequencies of 110.2 GHz and 164.4 GHz. As diode fabrication is improved to achieve lower series resistance, these loss factors will become significantly smaller.

IV. Control Impedance

Up to now [2], [14], monolithic beam control arrays have been designed for and tested under DC bias control. However, the arrays have broader application if they can operate at high control speed. To assess the control speed capability of the current array design, the 8640 diode array was tested with a low-frequency input modulation signal. The test configuration is shown in Fig. 13. A small-signal (0.6 V peak-to-peak) sinusoidal waveform was applied to a single bias unit of 8 × 60 diodes on the array (see Fig. 14). The control input signal was fed to the array mounting printed circuit board by a coaxial cable soldered to the edge of the board. The modulated power output detected from the array as a function of frequency is shown in Fig. 15. This behavior can be explained by a series RLC lumped element model of the control input circuit. The capacitance (24 pF) represents the sum of the individual diode capacitances and coplanar strip capacitance. The resistance (52 Ω) is an "average" value seen by an individual diode based on measured strip and diode resistances. It is primarily due to the "feed" strip which leads from the wirebond pad to the signal manifold on the opposite side of the array (see Fig. 14). The inductance (25 nH) is a similar "average" value which includes the coplanar strip inductance for the array and mounting board. (It has only a minor effect on the simulated performance, however.) The model provides a reasonable estimate of the observed behavior. The model indicates a 90% to 10% switching time of approximately 3 ns. The model suggests that the control speed of the array may be extendable by "overdriving" the array input signal. Furthermore, simple design modifications should provide a substantial speed improvement. For example, the resistance could be substantially reduced by feeding the control signal individually to each row pair, and by use of thicker bias metallization. Such changes should increase the control speed capability by at least a factor of four. Much higher control speed still should be possible by analysis and optimization of the coplanar strip feed structures as guided-wave paths.

At high control speed the generation of sidebands should be considered; these can be quantitatively considered by an

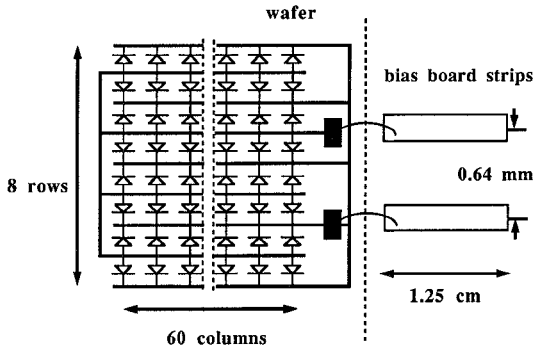

Fig. 14. Array layout for each array "bias unit".

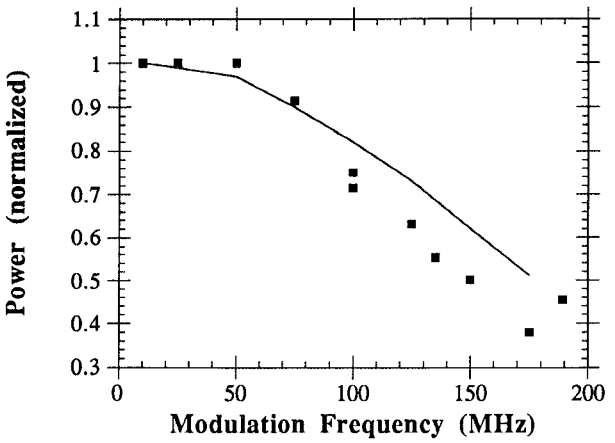

Fig. 15. Modulated power output versus control signal input frequency. Markers indicate experimental results (for a beam frequency of 158.7 GHz). The solid line indicates the predicted behavior based on the lumped element model of the control path.

analysis recently developed for arrays with embedded devices possessing a periodically-varying impedance [24]. A final observation on control operation is that if an array is designed specifically as a modulator, the diode doping profile can be tailored to provide the transmission versus bias relationship which produces the desired modulated beam waveform in response to the input waveform.

V. Conclusion

In this work, millimeter-wave Schottky diode array beam transmittance controllers with 4800 and 8640 devices have been demonstrated. The arrays show beam control in two "bands" in the vicinity of 100 GHz and 170 GHz, respectively. The 4800 diode array showed transmittance control over the range 20% to 50% at 99 GHz and 20% to 70% at 165 GHz.

An impedance parameter characterization was performed for the 8640 diode array. A de-embedding procedure was employed, in which model parameters were chosen to provide a curve-fit to a large set of transmission coefficient measurement results. The values obtained show good agreement with theoretical and low frequency results. If diodes with predictable dimensions can be fabricated, new array designs can be implemented with predictable operating parameters and performance. The primary factor which limited the predictability of the current arrays was the undercut of the wet etching process employed. For small-geometry devices, dry etching techniques are preferred due to their anisotropic etching behavior. Thus, the use of dry etching techniques for the diode arrays should largely address the need for predictability of performance.

Despite a relatively large quasi-optical resistance, (40 Ω) the array provides a substantial beam transmittance control. In contrast, this level of resistance precludes ([14]) efficient operation of the array as a reflection phase shifter. An incremental reduction of the array resistance should be possible by fabrication of an improved diode Ohmic contact. A much more dramatic improvement would be possible if an InP substrate-based Schottky diode can be employed.

The array capacitance shows a very low minimum quasi-optical capacitance, C_{min}, (about 5 fF), a hoped-for consequence of the use of the rectangular unit cell design. However, the quasi-optical capacitance (hence tuning) range is substantially reduced from that originally intended. This is due to two factors: First, the C-V range of the individual diodes is less than predicted. This is likely due to isolation implant penetration, which may be offset by higher doping or conversion to a mesa isolation process. Secondly, the quasi-optical capacitance range is less than that of the individual array diode. This is likely due to array defects, which should be largely eliminated when fabrication is performed on a routine basis. Since the diode dimensions of the current array are fairly large, scaling to smaller sizes should allow arrays which can operate to much higher ($\sim$ 1 THz) frequencies. Due to its tolerance of a large grid resistance, transmittance control should be considerably easier to accomplish at such frequencies than other quasi-optical functions.

The control frequency characterization indicates that the array, while designed for DC, shows no performance degradation up to 50 MHz. Minor design changes should allow this speed to be increased to 200–300 MHz, with much higher speeds possible with the control paths configured as optimized transmission line structures.

An example application (and one under active development) for such beam control is in the determination of magnetic fusion plasma density profiles. A millimeter-wave beam of a given frequency reflects from a plasma (cutoff) layer with a given electron density. Using a pulsed radar approach similar to the familiar ionospheric sounding technique, the reflection position in the plasma can be inferred from the round-trip group delay of the incident pulse. This allows the determination of the plasma density at one location, with the full profile obtainable from measurements performed at a number of different frequencies. A beam control array is employed to pulse the incident beam. With a pulse duration of 100 ps to 300 ps, such a system will provide the desired positional resolution for fusion reactors under development.

In the current work, we have demonstrated the capability of millimeter-wave beam transmittance control by a monolithic Schottky diode array. The experimental results and small-

signal characterizations should assist toward further array designs with enhanced performance. Advances in the development of array components, such as that of the current work, should contribute toward the eventual demonstration of complete systems based on solid state power-combining array technology.

ACKNOWLEDGMENT

This work was supported by Northrop Corporation under the University of California MICRO program. Additional support was provided by the U.S. Department of Energy, the Army Research Office, and the Joint Services Electronics Program, Contract No. F4962092-C-0055.

The authors would like to thank the staff of the JPL Microelectronics Devices Laboratory (in particular, R. Peter Smith) for access to device fabrication facilities and advice. Edith Baltram of Hewlett Packard ICBD (Corvallis) facilitated the donation of the wafer prober by ICBD to UCLA. MBE wafers of high quality have been provided by Leigh Florez and Jim Harbison of Bellcore, Inc., Prof. Christina Jou of NCTU (Taiwan), Prof. Mike Spencer of Howard University, and John Liu of JPL. Proton implantation was contributed by Michael Kroko (Kroko Engineering) and Rene Bernescot (Rockwell). Marko Sokolich (Hughes) performed the Ohmic contact alloying. Additional assistance to the work has been made by Clarence Becwar (Becwar Engineering), Larry Kapitan (QED), Matt Espiau and Misti Christianson (UCLA CHFE), Markus Van Loan (UCLA NFL), Charles Meng (UCLA), Prof. David B. Rutledge and Moonil Kim (Cal Tech), and Wayne Lam (Hughes), and Prof. R. J. Hwu, University of Utah.

REFERENCES

[1] J. W. Mink, "Quasi-optical power-combining of solid state millimeter-wave sources," *IEEE Trans. Microwave Theory Tech.,* vol. 34, no. 2, pp. 273–279, Feb. 1986.

[2] W. W. Lam, H. Z. Chen, K. S. Stolt, C. F. Jou, N. C. Luhmann, Jr., and D. B. Rutledge, "Millimeter-wave diode-grid phase shifters," *IEEE Trans. Microwave Theory Tech.,* vol. 36, no. 5, pp. 902–907, 1988.

[3] C. F. Jou, W. W. Lam, H. Chen, K. Stolt, N. C. Luhmann, Jr., and D. B. Rutledge, "Millimeter-wave monolithic Schottky diode-grid frequency doubler," *IEEE Trans. Microwave Theory Tech.,* vol. 36, no. 11, pp. 1507–1514, Nov. 1988.

[4] H-X. King, X-H. Qin, W. Wu, L. B. Sjogren, E. Chung, N. C. Luhmann, Jr., and W. A. Peebles, "Monolithic millimeter-wave quasi-optical frequency multiplier arrays," *Int. Semiconductor Device Research Symp. Proc.,* Dec. 1991, pp. 68–72.

[5] C. Zah, D. P. Kasilingam, J. S. Smith, D. B. Rutledge, T. Wang, and S. E. Schwartz, "Millimeter-wave monolithic Schottky diode imaging arrays," *Int. J. Infrared and Millimeter Waves,* vol. 6, pp. 981–997, 1985.

[6] Z. B. Popovic, R. M. Weikle, M. Kim, K. A. Potter, and D. B. Rutledge, "Bar grid oscillators," *IEEE Trans. Microwave Theory Tech.,* vol. 38, no. 3, pp. 225–230, Mar. 1990.

[7] Z. B. Popovic, R. M. Weikle, M. Kim, and D. B. Rutledge, "A 100-MESFET planar grid oscillator," *IEEE Trans. Microwave Theory Tech.,* vol. 39, no. 2, pp. 193–200, Feb. 1991.

[8] R. M. Weikle, M. Kim, J. B. Hacker, M. P. DiLisio, and D. B. Rutledge, "Planar MESFET grid oscillators using gate feedback," *IEEE Trans. Microwave Theory Tech.,* vol. 40, no. 11, pp. 1997–2003, Nov. 1992.

[9] M. Kim, J. J. Rosenberg, R. P. Smith, R. M. Weikle III, J. B. Hacker, M. P. Delisio, and D. B. Rutledge, "A grid amplifier," *IEEE Microwave Guided Wave Lett.,* vol. 1, no. 11, pp. 322–324, Nov. 1991.

[10] J. B. Hacker, R. M. Weikle II, M. Kim, M. P. DiLisio, and D. B. Rutledge, "A 100 element planar Schottky diode grid mixer," *IEEE Trans. Microwave Theory Tech.,* vol. 40, no. 3, pp. 557–562, Mar. 1992.

[11] J. Birkeland and T. Itoh, "A 16 element quasi-optical FET oscillator power combining array with external injection locking," *IEEE Trans. Microwave Theory Tech.,* vol. 40, no. 3, pp. 475–481, Mar. 1992.

[12] Paul E. Bakeman, Jr. and Albert L. Armostrong, "Fast, high power, octave bandwidth, X-band waveguide microwave switch," *IEEE MTT-S. Int. Microwave Symp. Dig.,* 1971, pp. 154–156.

[13] H-X. King, N. C. Luhmann, Jr., X-H. Qin, L. B. Sjogren, W. Wu, D. B. Rutledge, J. Maserjian, U. Lieneweg, C. Zah, and R. Bhat, "Millimeter-wave quasi-optical active arrays," *Proc. 2nd Int. Symp. on Space Terahertz Technology,* Feb., 1991, pp. 293–305.

[14] L. B. Sjogren, H-X. Liantz Liu, F. Wang, T. Liu, W. Wu, X-H Qin, E. Chung, C. W. Domier, N. C. Luhmann, Jr., J. Maserjian, M. Kim, J. Hacker, D. B. Rutledge, L. Florez, and J. Harbison, "Monolithic millimeter-wave diode array beam controllers: Theory and experiment," *Proc. 3rd Int. Symp. on Space Terahertz Technology,* Mar. 1992, pp. 55–67.

[15] K. D. Stephan and P. F. Goldsmith, "W-band quasioptical integrated PIN diode switch," *IEEE MTT-S Int. Microwave Symposium Dig.,* 1992, pp. 591–594.

[16] U. Lieneweg, T. J. Tolmunen, M. A. Frerking, and J. Maserjian, "Modeling of planar varactor frequency multiplier devices with blocking barriers," *IEEE Trans. Microwave Theory Techniques,* vol. 40, no. 5, pp. 839–845, May, 1992.

[17] L. B. Sjogren and N. C. Luhmann, Jr., "An impedance model for the quasi-optical diode array," *IEEE Microwave and Guided Wave Lett.,* vol. 1, no. 10, pp. 297–299, Oct. 1991.

[18] "HP85150A High-Frequency Structure Simulator," Hewlett-Packard Company, Network Measurements Division, Santa Rosa, CA.

[19] G. G. McFarlane, "Quasi-stationary field theory and its application to diaphragms and junctions in transmission lines and wave guides," *Proceedings Inst. Elec. Eng.,* vol. 93, Part IIIA, pp. 703–719, 1946.

[20] P. Waldow and I. Wolff, "The skin-effect at high frequencies," *IEEE Trans. Microwave Theory Tech.,* vol. 13, no. 10, pp. 1076–1082, Oct. 1985.

[21] D. Zhang, M. Matloubian, T. W. Kim, H. R. Fetterman, K. Chou, S. Prakash, C. V. Deshpandey, R. F. Bunshah, K. Daly, "Quasi-optical millimeter-wave band-pass filters using high-Tc superconductors," *IEEE Trans. Microwave Theory Tech.,* vol. 39, no. 9, pp. 1493–1497, Sept. 1991.

[22] H. H. Berger, "Models for contacts to planar devices," *Solid State Electron.,* vol. 15, no. 2, pp. 145–158, 1972.

[23] L. B. Sjogren, H-X. Liantz Liu, and N. C. Luhmann, Jr., "A polarization approach for quasi-optical phase measurement," *Microwave Optical Technology Lett.,* vol. 5, no. 12, pp. 623–627, Nov. 1992.

[24] L. W. Epp, C. H. Chan, and R. Mittra, "Periodic structures with time-varying loads," *IEEE Trans. Antennas Propagat.,* vol. 40, no. 3, pp. 251–256, Mar. 1992.

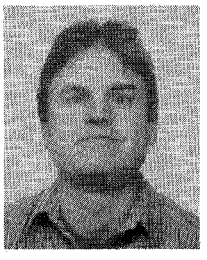

Lance Sjogren (M'86–S'86) was born in Portland, Oregon. In 1981, he received B.S. degrees in Electrical Engineering and Engineering Physics from Oregon State University. From 1981 to 1986, he worked as a Product Engineer and Packaging Development Engineer at Hewlett Packard Northwest Integrated Circuits Division. From 1986 to the present he has pursued graduate studies in Electrical Engineering at UCLA, completing the M.S. in 1989, with the PhD due to be completed in 1993. His research interests include the analysis and development of semiconductor device arrays for millimeter and submillimeter-wave beam control, amplification, and high power pulse generation.

Hong-Xia L. Liu, photograph and biography not available at the time of publication.

Feng Wang was born in Jiamusi, China on Aug. 10, 1969. She received the B.S. degree in Space Physics from Beijing University, China, in 1989, and the M.S. degree in Physics from the University of California, Los Angeles, in 1992. She is currently working for the M.S. and Ph.D. degrees in Electrical Engineering at the University of California, Los Angeles. The subject of her project is the optically activated beam control arrays.

Tina Y. Liu was born in Taipei, Taiwan on April 12, 1969. She received her B.S. degree in Electrical Engineering from National Tsing Hua University in 1991. She is presently a masters degree student in Electrical Engineering studying at the University of California, Los Angeles. The topic of her masters project is Millimeter-Wave Schottky Diode Amplitude Control Arrays.

Xiao-Hui Qin, photograph and biography not available at the time of publication.

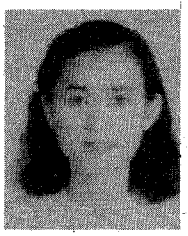

Wenhsing Wu received the B.S. degree in Electrophysics from the National Chiao Tung University, Taiwan in 1988 and the M.S. degree in Electrical Engineering from the University of California, Los Angeles in 1991. She is currently a Failure Analysis Engineer of the Mixed-Signal ICs at Silicon Systems in Tustin, California.

Esther I. Chung was born in Seoul, Korea on November 3, 1967. She received the B.S. degree in Electrical Engineering from University of California, Los Angeles in 1990. She is currently an M.S. candidate in Electrical Engineering at UCLA. Her thesis work involves the development of monolithic quasi-optical resonant tunneling diode (RTD) array frequency triplers in the millimeter-wave region. She has co-authored several papers on monolithic quasi-optical diode arrays.

Calvin W. Domier, photograph and biography not available at the time of publication.

N. C. Luhmann, Jr., photograph and biography not available at the time of publication.